Polymer(Korea), Vol. 40, No. 6, pp. 836-845 (2016)
http://dx.doi.org/10.7317/pk.2016.40.6.836

ISSN 0379-153X(Print)
ISSN 2234-8077(Online)

Basalt 단섬유로 보강된 POM 복합소재의 기계적 및 마찰 특성

Chenghe Liu*, Chunguang Long*,**,†, Lei Chen*, Junpeng Liu*, Taishan Cao*,**, and Jian Zhang*,**

*Institute of Automobile and Mechanical Engineering, Changsha University of Science and Technology
**Key Laboratory of Lightweight and Reliability Technology for Engineering Vehicle, College of Hunan Province

(2016년 2월 22일 접수, 2016년 4월 22일 수정, 2016년 7월 22일 채택)

Mechanical and Tribological Properties of Short Basalt Fiber-reinforced Polyoxymethylene Composites

Chenghe Liu*, Chunguang Long*,,†, Lei Chen*, Junpeng Liu*, Taishan Cao*,**, and Jian Zhang*,****

**Institute of Automobile and Mechanical Engineering, Changsha University of Science and Technology, Changsha-410114, Hunan, China*
***Key Laboratory of Lightweight and Reliability Technology for Engineering Vehicle, College of Hunan Province, Changsha-410114, Hunan, China*

(Received February 22, 2016; Revised April 22, 2016; Accepted July 22, 2016)

Abstract: In this paper, short basalt fiber-reinforced polyoxymethylene (POM) composites were prepared by melt blending and injection molding. The mechanical and tribological properties of the composites were studied by an orthogonal experiment. It was found that the optimal combination of fiber length 4 mm, fiber content 20 wt% and treated with KH550 would result in a comprehensive property which is 27.45% higher tensile strength, 9.65% higher impact strength and 18.11% higher flexural strength with compared to that of pure POM. But its tribological properties would be worse with the addition of the basalt fibers. After incorporating 10 wt% of polytetrafluoroethylene (PTFE) into the composites, the tribological properties of the composites was improved, closed to that of pure POM, with an insignificant decrease to their mechanical properties. Moreover, the morphology of fracture surfaces and worn surfaces evaluated by scanning electron microscopy showed good agreement with the results of the literature.

Keywords: basalt fibers, polyoxymethylene, mechanical properties, tribological properties.

Introduction

In recent years, the increasing interest in environmental issues has promoted the employment of natural fibers in polymer reinforcing.[1-4] Many types of natural fibers have been studied, such as sisal, flax, etc. However, vegetal fibers are very sensitive to thermal and hygroscopic load and show limited mechanical properties due to the fiber extraction system, the difficulty in fiber arrangement, the fiber dimension and the interface strength. A possible solution which overcomes the disadvantages of vegetal fibers, though taking into account the environmental issues, is represented by the use of natural mineral fibers, like basalt fibers (BF).

BF originated from volcanic rock[5] shows equivalent tensile strength, higher modulus and better alkaline resistance[6] compared with glass fiber. In addition, compared with carbon fiber,[7-9] BF has lower cost, higher flame retardance and more excellent thermal insulation. Therefore, in the last years continuous or short BF have been studied in view of their potential applications in polymer matrix composites.[9-16] Overall BF show several advantages, which make them a good alternative to glass fiber as a reinforcing material in composites used in several fields such as marine, automotive, sporting equipment, civil, etc. Czigány[17] asserted that the cheap basalt fiber can be efficiently applied in hybrid composite systems. They had already been adopted and studied as reinforcement in concrete matrix,[9] where their high temperature properties such as the high fire resistance were evidenced, or in polymer matrices like epoxy,[10] polypropylene[11-13] or phenol-formaldehyde resin.[14,15]

Polyoxymethylene (POM), with [-CH_2-O-] as the main chain,

†To whom correspondence should be addressed.
E-mail: 642426853@qq.com

is an engineering plastic with high mechanical strength, excellent abrasion resistance, fatigue resistance and moldability.[18,19] Nevertheless, up to now, lot of efforts have been devoted to further improving the mechanical strength of POM by means of incorporation with fillers such as calcium carbonate, talc, diatomite, clay, and glass fibers. Although different fillers reinforced POM composites have been reported,[20,21] the studies on short BF reinforced POM composites were scarcely reported.

In the present work, in order to achieve both better mechanical and tribological properties as bearing materials, the multifactor level of fiber length, content and surface treatment methods were optimized with the index of tensile strength, impact strength, flexural strength, friction coefficient and wear loss by orthogonal experiment.[4] After confirming the optimal combination, 10 wt% PTFE[22] would be added into the optimal combination to improve its tribological properties.

Experimental

Materials. POM (acetal copolymer) was purchased from Yunnan Yuntianhua Co., Ltd, China. Basalt fiber was supplied by Zhejiang GBF Basalt Fiber Co., Ltd, China. The different types of basalt fiber were: 11 μm-4 mm, 11 μm-3 mm, 13 μm-2 mm, 13 μm-1 mm. Sodium hydroxide (NaOH) was obtained from Tianjin Fengchuan Chemical Reagent Technology Co., Ltd, China. Acetic acid was obtained from Tianjin Xin Dayu Chemical Co., Ltd, China. Coupling agent (KH550) was obtained from Hara Yoshi Tian Yang Chemical Co., Ltd, China. Ethanol was supplied by Hengyang Kaixin Chemical Reagent Co., Ltd, China. Polytetrafluoroethylene (PTFE) was obtained from Dongguan Tianyang Plastic Materials Co., Ltd.

Design of Orthogonal Experiment. Orthogonal experiment is a method of multifactor level study, which is based on the orthogonal property from the comprehensive test to select part of the representative point test, the representative point with the homogeneous dispersion, neat comparable characteristics, and it is an efficient, economic experiment design method. It is known that the mechanical and tribological properties of a fiber reinforced polymer composite is primarily depend upon the fiber modulus and the modulus of the resin matrix, orientation of fiber, length of fiber and the content of the fiber.[23-25] One can also enhance the properties of basalt fiber composites by altering the surface, using this approach, the surface modification of basalt fiber can be achieved with improved mechanical and tribological results.[26] The purpose of the experiments' design was to investigate the impact strength, flexural strength, friction coefficient and wear loss of the composites by different fiber length, content and surface treatment methods. The three parameters were chosen as follows: A, fiber length; B, fiber content; C, fiber surface treatment methods. The details of the parameters and their values are given in Table 1.

Table 1. Factor Combinations of Orthogonal Experiment

Level no.	A (mm)	B (wt%)	C
1	1	5	C1
2	2	10	C2
3	3	20	C3
4	4	30	C4

C1: Untreated; C2: Treated with acetic acid; C3: Treated with KH550; C4: Treated with KH550 after treated with acetic acid.

Fiber Surface Modification. The orthogonal experiment scheme of fibers' different conditions is shown in Table 2. The blank column remaining in the column assignment is very important, since it can be used to record experimental error and indicate the reliability of the whole experiment.[27] There are four methods of pre-treatments: no-treatment, acetic acid treatment, KH550 treatment,[10] and acetic acid treatment followed by KH550 treatment.

Table 2. Orthogonal Experiment Scheme

Fiber no.	A Fiber length (mm)	B Fiber content (wt%)	C Surface treatment methods	D Blank column
1#	1	5	C1	1
2#	1	10	C2	2
3#	1	20	C3	3
4#	1	30	C4	4
5#	2	5	C2	3
6#	2	10	C1	4
7#	2	20	C4	1
8#	2	30	C3	2
9#	3	5	C3	4
10#	3	10	C4	3
11#	3	20	C1	2
12#	3	30	C2	1
13#	4	5	C4	2
14#	4	10	C3	1
15#	4	20	C2	4
16#	4	30	C1	3

Acetic Acid Treatment: BF were immersed in acetic acid solution (15 wt%) for 1.5 h at room temperature. Then the fibers were washed with distilled water containing a few drops of NaOH. Next, fibers were washed with distilled water until all acetic acid was eliminated, subsequently neutralized to pH 7. Finally, the fibers were dried in an oven at 100 °C for 5 h.

KH550 Treatment: For the surface treatment of the BF, 1.5 wt% KH550 (weight percentage compared to the fiber) was dissolved for hydrolysis in a mixture of water-ethanol (1:9 w/w), and stirred continuously for 0.5 h. Next, the fibers were soaked in the solution for 0.5 h. Finally, the fibers were dried in an oven at 120 °C for 4 h.

Acetic Acid Treatment and KH550 Treatment: BF were firstly treated by acetic acid solution as described in the acetic acid treatment step, and then by KH550 as described in the KH550 treatment step.

Composites Preparation. To ensure that all absorbed moisture was removed and to prevent void formation, the BF and the POM pellets were dried at 90 °C in an oven for 4 h before processing. The neat POM was melt compounded with the BF (on the orthogonal experiment) using a torque rheometer (Hapro RM 200A, Harbin, China) with a rotation speed of 35 r/min at 185 °C.

The specimen was prepared by injection molding at the specified temperature (185 °C) using an injection molding machine (LS-80, Liuzhou, China).

Mechanical Testing. Tensile Test: Specimens of the composites were tested for tensile strength according to GB/T 1040.1-2006 standard using a WDW-100C machine (Shanghai Hualong Test Instruments Co., Ltd, China). The shape and dimension of the specimen are shown in Figure 1. The tensile rate was 2 mm/min.

Impact Test: The impact strengths of the composites were carried out by a CBD-7.5 test machine (Shanghai Hualong Test Instruments Co., Ltd, China) according to GB/T 1043.1-2008. The impact velocity was 2.9 m/s and the impact energy was 4 J. Dimensions of the samples were 80×10×4 mm^3.

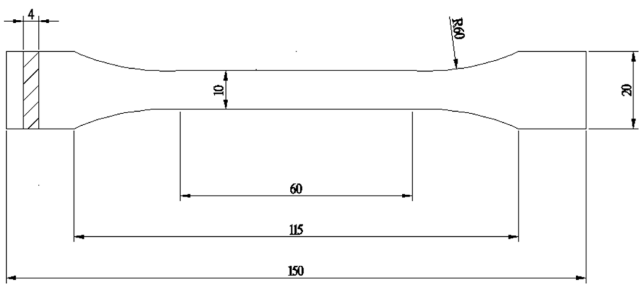

Figure 1. Shape and measurement of specimens (mm).

Flexural Test. The flexural properties of the composites were measured by a three-point bending method according to GB/T 9341-2008 standard using a WDW-100C Machine (Shanghai Hualong Test Instruments Co., Ltd, China). The crosshead speed was set at 2 mm/min. The dimension of flexural specimens was 80×10×4 mm^3.

Friction and Wear Test: The tribological tests of composites were conducted on a pin-on-disk test rig MMW-1 (Jinan Sida Instruments Co., Ltd, China) under dry condition (200 N, 1800 s, 200 r/min). Each sample was measured for its weight change on the electronic weighing balance XS205 (METTLER TOLEDO Corp., Ltd, China) which gave accuracy to 0.1 mg before and after the wear test. The tribological test for average friction coefficient and wear loss was repeated for three times. Before each testing, the surfaces of pins and specimen were cleaned with a soft paper containing ethanol to ensure proper contact of specimen with the counter-face.

Scanning Electron Microscopy: The morphologies of the impact-fractured surfaces and worn surfaces of the composites and the morphologies of fibers surfaces of BF were observed by scanning electron microscope (SEM) (Quanta 200 FEG, FEI Company) at room temperature. The samples were coated with gold using a vacuum sputter coater. The samples were viewed perpendicular to the detection surface.

Results and Discussion

Mechanical and Tribological Properties. Orthogonal Experiments Results and Discussions: The mechanical and tribological properties of composites are shown in Table 3. The result of mechanical properties was taken as the average of five test samples, and the result of tribological properties was taken as the average of three test samples.

The tensile strength of composites is shown in Table 3, range analysis in Table 4. It can be seen from Table 4 that the optimal combination for tensile strength is A4B4C2, namely: fiber length 4 mm, fiber content 30 wt% and treated with acetic acid. Figure 2 displays the correlation between the tensile strength of the composites and each factor of BF fibers. It should be noted that these graphs were only used to show the trends of each factor, not for predicting other values that were not tested experimentally. The tensile strength of composites is increased with increasing fiber length and content. As the fiber content is increased from 20 to 30%, the tensile strength of composites increases slightly. The main reasons are that the BF

Table 3. The Results of Orthogonal Experiment

Composite no.	A	B	C	D	Tensile strength (MPa)	Impact strength (10kJ/m^2)	Flexural strength (MPa)	Friction coefficient	Wearing capacity (mg)
1S	1	5	C1	1	54.07	26.600	180.66	0.303	3.1
2S	1	10	C2	2	55.75	26.347	184.87	0.296	3.6
3S	1	20	C3	3	60.66	27.969	183.92	0.301	4.6
4S	1	30	C4	4	58.06	29.001	175.13	0.320	8.6
5S	2	5	C2	3	56.88	25.423	179.70	0.287	2.1
6S	2	10	C1	4	61.76	26.028	196.08	0.289	3.6
7S	2	20	C4	1	63.50	28.456	183.06	0.311	4.7
8S	2	30	C3	2	65.79	29.122	170.96	0.332	5.9
9S	3	5	C3	4	56.60	27.879	198.75	0.310	4.3
10S	3	10	C4	3	58.29	28.001	205.95	0.311	4.1
11S	3	20	C1	2	62.36	28.654	214.82	0.328	4.9
12S	3	30	C2	1	75.77	28.120	271.62	0.330	7.9
13S	4	5	C4	2	59.24	26.897	216.60	0.279	2.7
14S	4	10	C3	1	63.48	27.656	226.56	0.288	3.1
15S	4	20	C2	4	74.20	28.450	264.02	0.323	8.1
16S	4	30	C1	3	71.82	28.620	284.04	0.335	8.0

Table 4. Range Analysis of Tensile Strength

Tensile strength (MPa)	Fiber length (mm)	Fiber content (wt%)	Surface treatment methods	Blank column
Mean 1	57.135	56.698	62.502	64.205
Mean 2	61.983	59.820	65.650	60.785
Mean 3	63.255	65.180	61.633	61.912
Mean 4	67.185	67.860	59.773	62.655
R	10.050	11.162	5.877	3.420
The best value	A4	B4	C2	D1

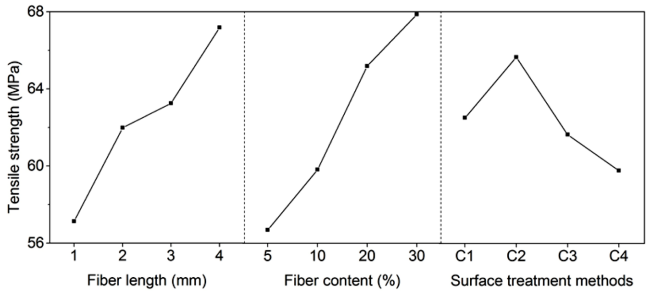

Figure 2. Relationship between each factor and tensile strength (Mean i, i=1, 2, 3, 4).

fibers in the composites can be used to support the load, and with the increase of fiber length and content, the load could be more effectively transferred from the matrix to the BF fibers to achieve good properties. The variance analysis is shown in Table 5. It can be concluded according to Table 5 that control factor B has the greatest impact on tensile strength followed by A and C.

The impact strength of composites is shown in Table 3, range analysis in Table 6. It can be seen from Table 6 that the optimal combination for impact strength is A3B4C3, namely: fiber length 3 mm, fiber content 30 wt% and treated with KH550. Figure 3 displays the correlation between the impact strength of the composites and each factor of BF fibers. With increasing fiber length up to 2 mm, the impact strength of the composites is decreased. In contrast, when the fiber length varies from 2 to 4 mm, the impact strength of the composites increases to the maximum value, then decreases. The impact strength of composites increases with the increase of fiber content, when the fiber content varies from 20 to 30%, the impact

Table 5. Variance Analysis of Tensile Strength

Sources of variance	Sum of squares of deviations, S	Freedom, γ	F	Fa	Notability
A	206.085	3	8.352	$F_{0.05}(3,3)=9.280$	
B	306.858	3	12.436		*
C	72.261	3	2.929		
D	24.674	3	1		
Error, E	24.67	3			
Sum, T	634.548	15			

Table 6. Range Analysis of Impact Strength

Impact strength (10kJ/m^2)	Fiber length (mm)	Fiber content (wt%)	Surface treatment methods	Blank column
Mean 1	27.479	26.700	27.476	27.708
Mean 2	27.257	27.008	27.085	27.755
Mean 3	28.164	28.382	28.157	27.503
Mean 4	27.906	28.716	28.089	27.840
R	0.907	2.016	1.072	0.337
The best value	A3	B4	C3	D4

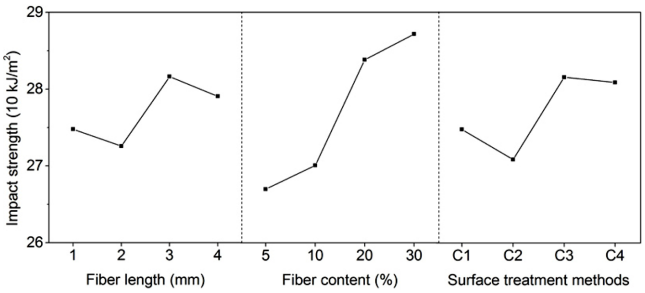

Figure 3. Relationship between each factor and impact strength (Mean i, i=1, 2, 3, 4).

strength of composites increases slightly. After the BF fibers was treated with acetic acid, the impact strength is decreased. The results are attributed to that the strength of BF fiber is decreased. After the BF fibers is treated with KH550, the impact strength increases. This is because it can form a film on the fibers surface with the appropriate concentration of KH550, which reduced the flaws on the fibers surface, played a reinforcing role to some extent (this was supported by SEM, as discussed in a subsequent section). The variance analysis is shown in Table 7. The B and C are the main factor affecting the impact strength, and the order of various factors that from important to minor on the impact strength is B, C and A.

The flexural strength of composites is shown in Table 3, range analysis in Table 8. It can be seen from Table 8 that the optimal combination for flexural strength is A4B4C2, namely: fiber length 4 mm, fiber content 30 wt% and treated with acetic acid. Figure 4 displays the correlation between the flexural strength of the composites and each factor of BF fibers. With increasing fiber length up to 2 mm, the flexural strength of

Table 7. Variance Analysis of Impact Strength

Sources of variance	Sum of squares of deviations, S	Freedom, γ	F	Fa	Notability
A	2.008	3	8.196	$F_{0.05}(3,3)=9.280$	
B	11.905	3	48.592		*
C	3.153	3	12.869		*
D	0.245	3	1		
Error, E	0.24	3			
Sum, T	17.551	15			

Table 8. Range Analysis of Flexural Strength

Flexural strength (MPa)	Fiber length (mm)	Fiber content (wt%)	Surface treatment methods	Blank column
Mean 1	181.145	193.793	218.900	215.475
Mean 2	182.450	203.365	225.053	196.678
Mean 3	222.785	211.455	195.048	213.402
Mean 4	247.670	225.438	195.050	208.495
R	66.525	31.645	30.005	18.797
The best value	A4	B4	C2	D1

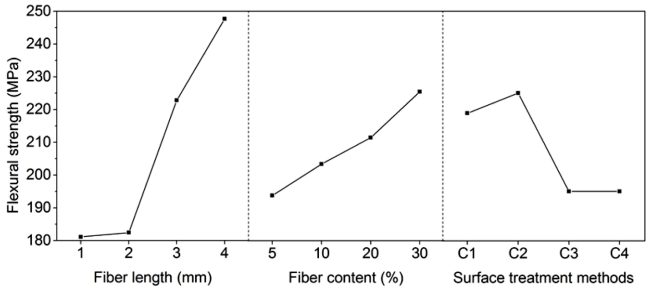

Figure 4. Relationship between each factor and flexural strength (Mean i, i=1, 2, 3, 4).

composites is hardly increased. In contrast, when the fiber length varies from 2 to 4 mm, the flexural strength of composites is significantly increased. Previous studies on the short fiber reinforced composites showed that the composite flexural strength increased as a function of fiber length.[28] The flexural strength of composites increases with the increase of fiber content. When the BF fibers is treated with acetic acid, the flexural strength obtains a maximum value. The variance analysis is shown in Table 9. It can be concluded according to Table 9 that control factor A has the greatest impact on the flexural strength followed by C and B.

The friction coefficient of composites is shown in Table 3, range analysis in Table 10. It can be seen from Table 10 that the optimal combination for friction coefficient is A1A2B1C4, namely: fiber length 1 mm or 2 mm, fiber content 5 wt% and treated with KH550 after treated with acetic acid. Figure 5 displays the correlation between the friction coefficient of the composites and each factor of BF fibers. In addition to a sharp increase at 3 mm, the friction coefficient changed little with the increase of fiber length. With increasing fiber content up to 10%, the friction coefficient of composites is hardly increased.

Table 9. Variance Analysis of Flexural Strength

Sources of variance	Sum of squares of deviations, S	Freedom, γ	F	Fa	Notability
A	12660.992	3	14.898	$F_{0.05}(3,3)=9.280$	*
B	2153.156	3	2.534		
C	2976.068	3	3.502		
D	849.824	3	1		
Error, E	849.82	3			
Sum, T	19429.860	15			

Table 10. Range Analysis of Friction Coefficient

Friction coefficient	Fiber length (mm)	Fiber content (wt%)	Surface treatment methods	Blank column
Mean 1	0.305	0.295	0.314	0.317
Mean 2	0.305	0.296	0.309	0.313
Mean 3	0.320	0.316	0.308	0.300
Mean 4	0.306	0.329	0.305	0.306
R	0.015	0.034	0.009	0.017
The best value	A1,A2	B1	C4	D3

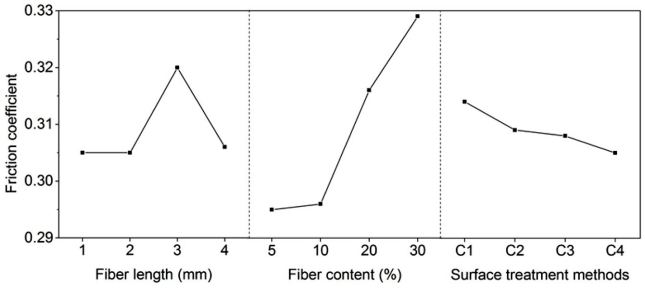

Figure 5. Relationship between each factor and friction coefficient (Mean i, i=1, 2, 3, 4).

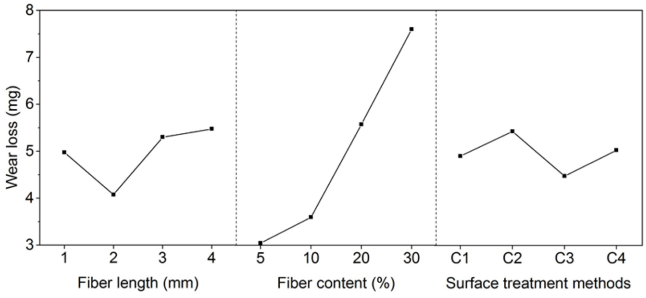

Figure 6. Relationship between each factor and wear loss (Mean i, i=1, 2, 3, 4).

In contrast, when the fiber content varies from 10 to 30%, the friction coefficient of composites is significantly increased. Surface modifications on BF fibers can effectively decrease the friction coefficient of the composites. The variance analysis is shown in Table 11. It can be concluded according to Table 11 that these factors have limited impact on the friction coefficient, and the order of various factors that from important to minor on the impact strength is B, A and C.

The wear loss of composites is shown in Table 3, range analysis in Table 12. It can be seen from Table 12 that the optimal combination for wear loss is A2B1C3, namely: fiber length 2 mm, fiber content 5 wt% and treated with KH550. Figure 6 displays the correlation between the wear loss of the composites and each factor of BF fibers. It can be found that the BF fibers would sharply increase the wear loss of the composites so as to decrease the composites' wear resistance. The wear loss of the composites decreases with the fiber length increasing from 1 to 2 mm, and increases from 2 to 4 mm. The wear loss of the composites increases with the increase of fiber content, when the fiber content varies from 10 to 30%, the wear loss of the composites is significantly increased. This may be due to that more BF fibers would be dropped out from the matrix with the increase of fiber content. They act as a third body abrasion between the surface of the steel pin and the composite disk which causes an increasing of the wear loss. When the BF fibers treated with KH550, the wear loss obtained a minimum value. The variance analysis is shown in Table 13. It can be concluded according to Table 13 that control factor B has the greatest impact on flexural strength followed by A, C.

Table 11. Variance Analysis of Friction Coefficient

Sources of variance	Sum of squares of deviations, S	Freedom, γ	F	Fa	Notability
A	0.001	3	1.000	$F_{0.05}(3,3)=9.280$	
B	0.003	3	3.000		
C	0.000	3	0.000		
D	0.001	3	1.000		
Error, E	0.00	3			
Sum, T	0.005	15			

Table 12. Range Analysis of Wear Loss

Wear loss (mg)	Fiber length (mm)	Fiber content (wt%)	Surface treatment methods	Blank column
Mean 1	4.975	3.050	4.900	5.300
Mean 2	4.075	3.600	5.425	5.150
Mean 3	5.300	5.575	4.475	4.700
Mean 4	5.475	7.600	5.025	4.675
R	1.400	4.550	0.950	0.625
The best value	A2	B1	C3	D4

Table 13. Variance Analysis of Wear Loss

Sources of variance	Sum of squares of deviations, S	Freedom, γ	F	Fa	Notability
A	4.657	3	3.874	$F_{0.05}(3,3)$=9.280	
B	51.382	3	42.747		*
C	1.837	3	1.528		
D	1.202	3	1		
Error, E	1.20	3			
Sum, T	60.278	15			

Optimal Combination (OC): According to the orthogonal experiment, the fiber length is the main factor affecting the flexural strength, and the best option is A4. The fiber content is the main factor affecting the tensile strength, impact strength and wear loss. When the fiber content varies from 20 to 30%, the tensile strength and impact strength increase slightly, while the wear loss significantly increases. From the results above, we take B3 as the best option. The surface treatment methods is the main factor affecting the impact strength, and the best option is C3. The optimal combination for comprehensive properties is A4B3C3, namely: fiber length 4 mm, fiber content 20 wt% and treated with KH550. The mechanical and tribological properties of OC and pure POM are shown in Table 14. We can see that the OC displays a 27.45% higher tensile strength, a 9.65% higher impact strength and an 18.11% higher flexural strength than the pure POM. However, the OC displays a 16.86% higher friction coefficient and a 77.78% higher wear loss than the pure POM.

Optimal Combination Adding 10 wt% PTFE (OCP): After confirming the optimal combination, 10 wt% PTFE would be added into the optimal combination to improve its tribological properties. The mechanical and tribological properties of OCP are shown in Table 14. We can see that the friction coefficient and wear loss of OCP is close to pure POM, the impact strength of OCP is close to OC. However, the OCP displays a 7.12% lower tensile strength and a 9.83% lower flexural strength than OC. The main reasons are that

Morphological Analysis Results. Initially, SEM analysis performed on the BF fibers highlights the relevance of treating

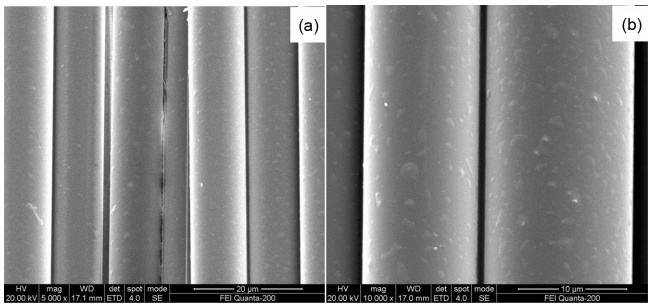

Figure 7. SEM micrographs of the surface of BF fibers treated with KH550, scale bar: (a) 20 μm (5000×); (b) 10 μm (10000×).

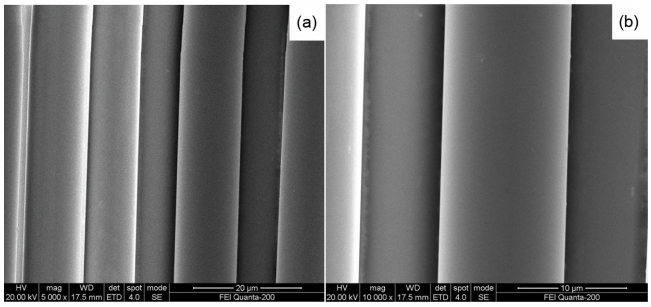

Figure 8. SEM micrographs of the surface of BF fibers, scale bar: (a) 20 μm (5000×); (b) 10 μm (10000×).

with KH550 on the surface microstructure of basalt fibers. In facts, the fibers treated with KH550 are characterized by a rough surface (Figure 7). In contrast, untreated basalt fibers are characterized by a very smooth and clean surface, as evidenced by the micrograph reported in Figure 8. It can form a film on the fibers surface with the appropriate concentration of

Table 14. Mechanical and Tribological Properties of Optimal Combination and Pure POM

Materials	Tensile strength (MPa)	Impact strength (10 kJ/m^2)	Flexural strength (MPa)	Friction coefficient	Wear loss (mg)
OC	67.83	28.601	215.37	0.305	6.4
OCP	63.00	28.423	194.20	0.258	3.5
Pure POM	53.22	26.084	182.34	0.261	3.6

KH550, which reduced the flaws on the fibers surface, played a reinforcing role to some extent. In order to further clarify this issue, the FTIR spectroscopy was used to confirm the chemical reactions between KH550 and the fibers. Wang *et al*.,[29] reported FTIR spectra of the untreated and treated BF fibers. They found that the spectrum of KH550 as consisting of several peaks, appearing at the 3356, 2927, 1085, 1002 and 916 cm^{-1} wave numbers, respectively. The spectrum of BF fibers treated with KH550 as consisting of several peaks, appearing at the 880 cm^{-1} corresponding to silicon-based compoundands and 724 cm^{-1} corresponding to Si-O. Combined with Figure 7, there is coupling agent stay on the surface of the fibers that treated with KH550. However, Si-O-Si and other peaks of KH550 does not appear in the FTIR spectra of the treated BF fibers, indicating KH550 does not react with the BF fibers. This may have been due to that smaller content KH550 adhered to the surface of BF fibers, the absorption peak would be masked and difficult to characterize.

The fracture surface morphology of pure POM, OC and OCP is analyzed by SEM as shown in Figure 9 to 11. Most of the fibers are pulled-out, leaving circular holes in the matrix (Figure 10, Figure 11), compared with the pure POM, the BF fibers in the composites can be used to support the load. The broken fibers in the fracture interface indicated that load was effectively transferred from the matrix to the BF fibers to achieve good properties. Failure occurs at the fiber matrix interface. The fibers surfaces appear clean and smooth, indicating that the interfacial bonding between matrix and BF fibers is insufficient to provide satisfactory reinforcement in the composites. The processing of the composites results in a dispersed morphology of the fibers. The good dispersion of fibers into the polymeric matrix ensures a reduction in the composites anisotropy, reflecting directly in the transfer load ability. Figure 11 presents SEM photomicrographs of the fracture surface of the OCP, we can see that most of the fibers has a good combination with the matrix, but a few of them (remarked by 1) shows a weak interface between POM and PTFE.

Figure 12 shows SEM photomicrographs of the wear scars of pure POM, OC and OCP. It can be seen that the worn surface is smooth, and only exhibits fine scratches, there are a few ribbon like tears and pieces of debris on the scars. They are the typical debris generated by adhesive wear. So the worn surface of pure POM is characterized by plastic deformation and adherence (Figure 12(a)). Many scratch grooves are clearly observed on the worn scars of OC (Figure 12(b)). In addition, the phenomenon of thermal softening is obviously present on

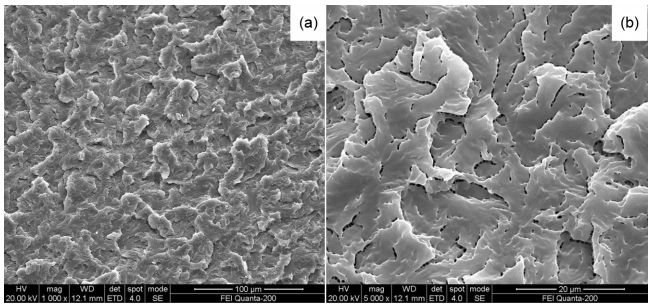

Figure 9. SEM micrographs of the fracture surface of pure POM, scale bar: (a) 100 μm (1000×); (b) 20 μm (5000×).

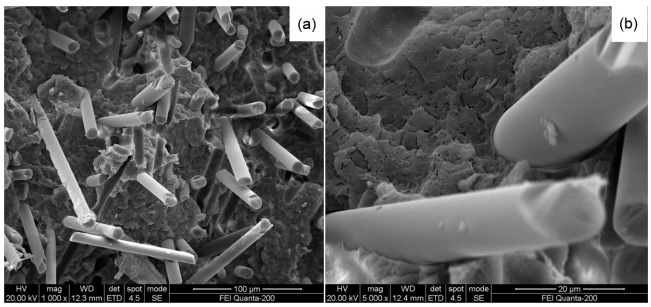

Figure 10. SEM micrographs of the fracture surface of optimal combination composites, scale bar: (a) 100 μm (1000×); (b) 20 μm (5000×).

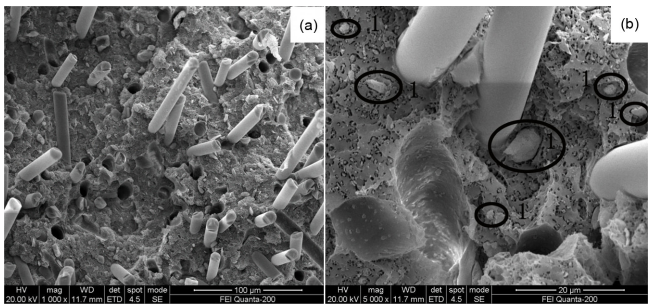

Figure 11. SEM micrographs of the fracture surface of optimal combination composites adding 10 wt% PTFE, scale bar: (a) 100 μm (1000×); (b) 20 μm (5000×).

the worn surface. By adding the BF fibers, a lot of broken fibers are present in the contact surface. They act as a third body abrasion between the surface of the steel pin and the composite disk which causes an increasing of the friction coefficient and wear loss. Hence, the wear mechanism is plastic deformation and grain- abrasion. In Figure 12(c) which shows the wear scars of the OCP, the signs of delamination, including material folding and separations can be clearly observed. There are large-stripped and layered spallings and some ribbon like tears and pieces of debris almost on the verge of detachment.

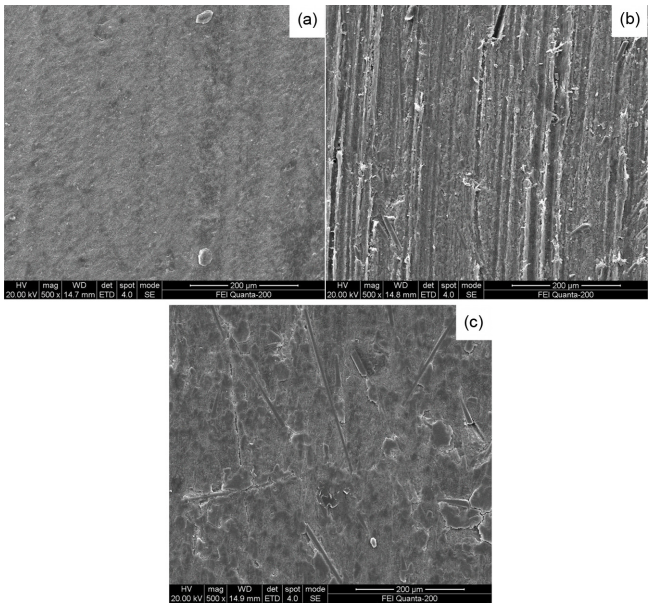

Figure 12. SEM micrographs of the worn surfaces of POM and its composites: (a) pure POM; (b) optimal combination composites; (c) optimal combination composites adding 10 wt% PTFE; scale bar: (a) 200 μm (500×); (b) 200 μm (500×); (c) 200 μm (500×).

It is the typical debris generated by adhesive wear. Then, in the following sliding, the large pieces of debris were extruded and broken into little pieces or block debris, and a part of them is adsorbed on the surfaces of BF fibers to reduce the damage of the fibers. Thereby, the wear is reduced. Overall, because of the above reasons, by adding PTFE, the friction coefficient and wear loss of the OCP composites are decreased obviously.

Conclusions

In this work, the short basalt fiber-reinforced POM composites were prepared by melt blending and injection molding technique. The mechanical and tribological properties of the composites were investigated by an orthogonal experiment. The results show that the composites got the best comprehensive properties when the BF fibers achieved these conditions: fiber length 4 mm, fiber content 20 wt% and treated with KH550. The mechanical properties of the composites could be improved significantly with a suitable adding of BF fibers, however, its tribological properties would be worse compared with that of the pure POM. After a 10 wt% of PTFE into the composites, the tribological properties of the composites could also be improved obviously, and with an insignificant decrease to their mechanical properties. The SEM photographs of fracture surfaces and wear scars of composites clearly indicated the extent of fiber-matrix interface adhesion, and different wear mechanisms on the worn surfaces.

Acknowledgments: This work is supported by the Key Scientific Research Foundation of Education Department of Hunan Province (No. 14A011), and the Key International and Regional Scientific and Technological Cooperation Project of Hunan Province (2014WK2035).

References

1. P. Anand and V. Anbumalar, *Polym. Korea*, **39**, 46 (2015).
2. V. Lopresto, C. Leone, and I. D. Iorio, *Compos. Part B-Eng.*, **42**, 717 (2011).
3. P. Anand and V. Anbumalar, *Polym. Korea*, **30**, 347 (2011).
4. Y. Zhou, C. Long, J. Huang, Z. Deng, and T. Cao, *J. Reinf. Plast. Compos.*, **32**, 1348 (2013).
5. T. Czigány, J. Vad, and K. Pölöskei, *Mech. Eng.*, **49**, 3 (2005).
6. F. Kajzar, E. M. Pearce, N. A. Turovskij, and O. V. Mukbaniani, "Interdisciplinary Concepts and Research," in *Key Engineering Materials*, CRC Press, Florida, Vol **2** (2014).
7. A. A. Dalinkevich, K. Z. Gumargalieva, S. S. Marakhovsky, and A. V. Soukhanov, *J. Nat. Fibers*, **6**, 248 (2009).
8. T. Czigány, K. Pölöskei, and J. Karger-Kocsis, *J. Mater. Sci.*, **40**, 5609 (2005).
9. J. Sim, C. Park, and D. Y. Moon, *Compos. Part B-Eng.*, **36**, 504 (2005).
10. M. S. Kim and S. J. Park, *Polym. Korea*, **39**, 219 (2015).
11. S. Matkó, P. Anna, G. Marosi, A. Szép, S. Keszei, T. Czigány, and K. Pölöskei, *Macromol. Symp.*, **202**, 255 (2003).
12. T. Czigány, *Mater. Sci. Forum*, **473**, 59 (2004).
13. P. I. Bashtannik, V. G. Ovcharenko, and Y. A. BootMech, *Compos. Mater.,* **33**, 600 (1997).
14. S. Ozturk, *J. Mater. Sci.*, **40**, 4585 (2005).
15. S. E. Artemenko, *Fibre. Chem.*, **35**, 226 (2003).
16. M. Wang, Z. Zhang, Y. Li, M. Li, and Z. Sun, *J. Reinf. Plast. Compos.*, **27**, 393 (2008).
17. T. Czigány, *Compos. Sci. Technol.*, **66**, 3210 (2006).
18. S. Hasegawa, H. Takeshita, F. Yoshii, T. Sasaki, K. Makuuchi, and S. Nishimoto, *Polymer*, **41**, 111 (2000).
19. H. Hisakatsu and T. Kohji, *Polymer*, **44**, 3107 (2003).
20. K. Kawaguchi, K. Mizuguchi, K. Suzuki, H. Sakamoto, and T. Oguni, *J. Appl. Polym. Sci.,* **118**, 1910 (2010).
21. Z. Qian, Y. Wang, J. Li, X. Wang, and D. Wu, *J. Reinf. Plast. Compos.,* **33**, 294 (2014).
22. C. Long, *Lubr. Eng.,* **36**, 41 (2011).
23. Y. Zhang, C. Yu, P. K. Chu, F. Lv, C. Zhang, J. Ji, R. Zhang, and H. Wang, *Mater. Chem. Phys.*, **133**, 845 (2012).
24. H. Fukuda and T. W. Chou, *J. Mater. Sci.*, **17**, 1003 (1982).
25. P. A. Templeton, *J. Reinf. Plast. Compos.*, **9**, 210 (1990).
26. M. T. Kim, M. H. Kim, K. Y. Rhee, and S. J. Park, *Compos. Part B-Eng.*, **42**, 499 (2011).
27. X. Wu and D. Y. C. Leung, *Appl. Energ.*, **88**, 3615 (2011).
28. H. Zhang, Z. Zhang, and K. Friedrich, *Compos. Sci. Technol.*, **67**, 222 (2007).
29. W. Wang and G. J. Lu, *Acta Mater. Compos. Sin.*, **30**, 315 (2013).